Soy protein–nanocellulose composite aerogels

ARTICLE *in* CELLULOSE · OCTOBER 2013

Impact Factor: 3.57 · DOI: 10.1007/s10570-013-9993-4

Cellulose (2013) 20:2417–2426
DOI 10.1007/s10570-013-9993-4

ORIGINAL PAPER

Soy protein–nanocellulose composite aerogels

Julio C. Arboleda · Mark Hughes · Lucian A. Lucia · Janne Laine · Kalle Ekman · Orlando J. Rojas

Received: 9 March 2013 / Accepted: 5 July 2013 / Published online: 13 July 2013

Abstract Organic aerogels based on two important and widely abundant renewable resources, soy proteins (SP) and nanofibrillar cellulose (NFC) are developed from precursor aqueous dispersions and a facile method conducive of channel- and defect-free systems after cooling and freeze-drying cycles that yielded apparent densities on the order of 0.1 g/cm^3. NFC loading drives the internal morphology of the composite aerogels to transition from network- to fibrillar-like, with high density of interconnected cells. Composite aerogels with SP loadings as high as ca. 70 % display a compression modulus of 4.4 MPa very close to that obtained from reference, pure NFC aerogels. Thus, the high compression modulus of the composite system is not compromised as long as a relatively low amount of reinforcing NFC is present. The composite materials gain moisture (up to 5 %) in equilibrium with 50 % RH air, independent of SP content. Furthermore, their physical integrity is unchanged upon immersion in polar and non-polar solvents. Fast liquid sorption rates are observed in the case of composite aerogels in contact with hexane. In contrast, water sorption is modulated by the chemical composition of the aerogel, with an important contribution from swelling. The potential functionalities of the newly developed SP–NFC composite green materials can benefit from the reduced material cost and the chemical features brought about the amino acids present in SPs.

Keywords Composite aerogels · Soy proteins · Nanocellulose · Cellulose nanofibrils · Freeze casting · Nanofibrillated cellulose · Microfibrillated cellulose (MFC) · NFC · Porous solids

Electronic supplementary material The online version of this article (doi:10.1007/s10570-013-9993-4) contains supplementary material, which is available to authorized users.

J. C. Arboleda · L. A. Lucia · O. J. Rojas (✉)
Department of Forest Biomaterials, North Carolina State University, 2820 Faucette Drive, Raleigh, NC 27695-8005, USA
e-mail: ojrojas@ncsu.edu

M. Hughes · J. Laine · O. J. Rojas
Department of Forest Products Technology, School of Chemical Technology, Aalto University, P. O. Box 16300, 00076 Aalto, Espoo, Finland

L. A. Lucia
Department of Chemistry, North Carolina State University, Dabney Hall, 2620 Yarbrough Drive, Raleigh, NC 27695-8204, USA

K. Ekman
Stora Enso Biomaterials, Pulp Competence Centre, 55800 Imatra, Finland

Introduction

Residual soy proteins (SPs), a by-product of the soy oil industry are currently utilized in applications such as animal feed and their valorization as food supplement is currently being pursued. The growing soy oil demand and concurrent anticipated availability of

these inexpensive, residual SPs have stimulated interest in developing new functional materials. This is mainly because of the fact that beyond its abundance and nutritional value, SPs possess valuable properties such as biodegradability and biocompatibility; they also display a multiplicity of chemical functionality, amphoteric behavior, and pH responsiveness (Endres 2001).

It has been shown that SPs can be used in adhesives (Zhong et al. 2007), films (Song et al. 2011), gels (Renkema et al. 2000), emulsions (Wagner and Gueguen 1999), and can be adsorbed on both hydrophilic and hydrophobic materials to modulate their surface energy and chemical composition (Goli et al. 2012; Salas et al. 2012). SPs can be also used for medical applications to reduce oxidative stress, tissue engineering, drug delivery, etc. (Reddy and Yang 2011; Sarmadi and Ismail 2010).

In general, the field of aerogels is quite broad and encompasses a number of templating materials that include inorganic-based porous materials. Because of their distinctive properties such as low density, high surface area and low thermal conductivity, these materials can be used in the design of thermal insulators (Gurav et al. 2010), porous catalysts for chemical processes (Gurav et al. 2010; Menzel et al. 2012; Zhang and Riduan 2012) and porous ceramics for filtration and separation (Luyten et al. 2010). Additionally, polymer-based aerogels are of interest given their enhanced low density and high porosity (for example, Styrofoam^{TM}) and also because of their sorption capacity that has proven useful in the abatement of oil spills (Korhonen et al. 2011).

In this study, SPs were investigated for the development of aerogels based upon a process of controlled solvent removal from respective precursor aqueous dispersions. The use of such materials for aerogels is not unprecedented; for example, wheat proteins, which to some extent are similar to SPs in terms of amino acid composition, have been reported for the fabrication of solid foams (Blomfeldt et al. 2010).

Practical uses of SPs in the development of solid materials is nevertheless very challenging because they tend to be brittle and possess limited mechanical strength. Therefore, nanofibrillar cellulose (NFC) was used as reinforcing phase to enhance the mechanical properties of the material. In this way, this article provides the first documented study of not only SP-based aerogels, but the introduction of reinforcing NFC as an emerging new materials. NFCs are a biodegradable fibrous material with superior strength that have shown promise for a gamut of purposes (Khalil et al. 2012) and can interact strongly with SP, as demonstrated in our previous work (Salas et al. 2012). Relevant to this work is the use of NFC to develop porous solids (Paakko et al. 2008), hydrophobic aerogels for oil adsorption (Granström et al. 2011; Korhonen et al. 2011), magnetic aerogels as elements in actuators (Olsson et al. 2010), photoswitchable absorbents (Kettunen et al. 2011), cargo carriers on water and oil (Jin et al. 2011), and supported catalysts based on metal nanoparticles (Koga et al. 2012).

Despite the ostensible benefits of NFC when used alone or as the main component in an aerogel, this research also suggests that the resultant properties of SP-based aerogels can achieve commensurate materials properties of NFC-based aerogels when a relatively low amount of NFC is introduced in the context of a composite system. Not only can SPs allow for a reduced material cost, but they can endow the resultant structures with new chemical functionalities and different morphologies. Overall, SP–NFC composite porous materials are fully based on widely available and sustainable resources, can be developed via green processes, and compete favorably in conventional applications dominated by petroleum-based materials.

The inherently potential attractive properties of the proposed composite aerogels are their morphology and properties such as specific surface area, liquid sorption, mechanical strength, etc., all of which are highly dependent on the production method used. In this regard, several techniques have been applied (Luyten et al. 2010). The most common and generic methods involve homogeneous dispersions or solutions in a solvent that is subsequently removed by drying. However, a limitation is that conventional drying via heating involves large capillary forces that dominate during meniscus formation, which induces the collapse of the porous structure. As a result, supercritical and freeze drying are preferred methods for solvent removal because they involve lower mechanical stresses. Evidently, the formation of homogeneous porous structures demands precursor systems capable of withstanding stresses that develop upon solvent removal at a given solids content.

Freeze drying, which is the method used in this work, uses a dispersion, an aqueous gel, or a solution

which is frozen. The solvent is removed by sublimation under high vacuum; by using this technique, the spaces vacated by the solvent crystals become pores. The morphology of the crystals depends on the freezing conditions or the specific cooling protocol used (cooling rate and pressure, mainly) which thus impacts the structure of the final porous aerogel. For example, fast freezing by using liquid nitrogen or liquid propane, has been used to produce aerogels (Korhonen et al. 2011; Paakko et al. 2008). In such cases water (or the given solvent) solidifies very quickly and triggers a very extensive crystal nucleation in which the actual crystal growth is limited; hence, porous structures with pore diameters in the range of 1–60 nm can be produced.

The present manufacturing method involved freeze drying aqueous systems at slow cooling rates which overcame the following hurdles that are otherwise typical: (1) presence of stresses from fast expansion upon crystallization, which result in cracks; (2) the use of liquid nitrogen or propane that make scale up difficult and, (3) temperature gradients within the sample that induce heterogeneities and limit the dimensions of the material that is processed.

Materials and methods

Soy protein (SP) gels were prepared from ProFam 955, a commercial soy protein isolate with 90 % protein concentration and kindly supplied by ADM (Decatur, IL). This material is typically produced by grinding and screening soybean flakes after removal of oil followed by extraction (aqueous solution, pH 8–9) and adjustment of pH to 4.5, where most of the protein precipitates as a curd, which is finally washed and spray-dried. As a result, one-third of the starting flake weight is recovered in the form of a soy protein isolate.

NFCs were prepared from bleached elemental chlorine free kraft wood fibers produced from birch (*Betula pendula*) and provided as a never dried pulp with a solids content of approximately 20 % (w/w). NFC was produced by grinding the pulp with an ultrafine friction grinder Masuko Super Masscolloider MKZA 10-15 J (Masuko Sangyo Co. Ltd., Japan) equipped with SiC grinding stones (MKE 10-46). The grinding stone gap was 100 μm, and the pulp solids content was 1.3 % (w/w). The pulp was passed five times through the grinding chamber, using a total net specific energy consumption of 20 MWh t^{-1}. The resultant NFC gel was concentrated into a dispersion with 9 % solids content upon centrifugation at 12,000 rpm for 1 h four times (Beckman Coulter Optima L-90K Ultracentrifuge with a 70 Ti rotating head).

Preparation of the aerogels

A 10 % SP gel was prepared by diluting SP isolate in 0.1 N HCl followed by heating to 70 °C under stirring for 1 h; use of this procedure resulted in a viscous protein gel. The protein gel was easily mixed using a spatula with NFC (9 %) suspension, 1 N HCl, and water to obtain hydrogels with 8 % final total solid content, 0.09 N HCl concentration, and NFC:SP ratios ranging from 0:100 to 100:0. These mixtures were cast in plastic molds (10 × 10 × 40 mm dimension). The samples were then cooled in a refrigerator to 13 °C and after 1 h they were placed in a freezer set at −10 °C. Finally, the frozen samples were dried in an Edwards micro Modulyo Freeze dryer (Crawley, West Sussex, UK). The specimens developed some protrusions at the ends of the molds caused by material expansion upon water crystallization. Therefore, any excess material protruding from the walls of the mold was removed with a cutter to obtain specimens with known, precise dimensions. The aerogels were finally stored in a desiccator with silica gel until use.

Physical characterization

The apparent density was obtained from the dry mass and volume of the given aerogel sample. Tomography analysis was performed by using a 1072 SkyScan X-ray microtomograph (Skyscan, Belgium). Surface BET area was obtained by using a Micromeritics Gemini VII surface area analyzer (Micromeritics, USA) using glass beads to reduce the free space. The dry aerogel samples were conditioned in a room with constant temperature (23 °C) and relative humidity (50 %) and weighted after 48 h to determine their equilibrium moisture content.

Mechanical properties

The mechanical properties of the conditioned samples were evaluated by compression tests using a MTS 400M Test machine operated with a 200 N load cell

(at a compression rate of 1 mm/min). The samples were placed horizontally and the compressive force applied to one of the long sides of the aerogel sample.

Water sorption

Samples of the aerogels were suspended vertically in a KSV Instruments Tensiometer (model Sigma 70m Helsinki, Finland). In a typical experiment, a container filled with water or hexane was placed underneath the sample, which was advanced towards the liquid surface until contact. As a consequence, the fluid rose through the porous material (via wicking) and the weight gain recorded as a function of time while keeping the immersion depth constant (so that buoyancy effects were accounted for). The square of the adsorbed mass was then correlated to contact time according to the simple form of the Washburn equation for wetting of porous solids (Washburn 1921).

Results and discussion

By using the method introduced in the Experimental section, homogenous aerogels were obtained from pure SP and NFC and also from their mixtures (Fig. 1). The SP aerogels presented an off-white color, while those obtained from pure NFC were brighter. The SP materials were brittle and produced dust upon cutting; in contrast, the NFC aerogels were rigid. The brittleness of SP-based aerogels disappeared or was extensively reduced by addition of NFC loading, i.e., in composite aerogels.

The native globular structure of SPs prevents the formation of continuous structures such as films, gels, or porous materials. Therefore, to better process SPs, they have to be denatured to open up their globular structure and facilitate the formation of polymer networks. Thus, SPs were first thermally denatured in acidic conditions to form a reversible gel (Renkema et al. 2000).

The prepared samples shrank upon drying, which was more evident at the ends of the specimen where the expansion by freezing was less restricted by the rigid walls of the open-ended rectangular mold. The original short-side dimension of 10 mm was reduced by about 1 mm after drying (to 8.99 ± 0.14 mm, equivalent to a 27 % volume shrinkage). The shrinkage facilitated the removal of the aerogel sample from the mold. This was especially helpful in the case of aerogels from pure SPs that were brittle and more prone to damage during their removal.

Aerogel morphology

Images from tomographic scans for three selected aerogels, obtained from pure SP, pure NFC, and a SP–NFC 50:50 composite, are shown in the lower section of Fig. 1. Tomographic images of SP and NFC aerogels confirm the presence of extensive void spaces; however, in the case of SP the pores seem to be more interconnected and have loosely-defined cell edges. However, the differences in structure are difficult to determine with precision given the low resolution of the micro tomographic images. Nevertheless, the resultant mechanical properties of the material change considerably, as will be discussed later. High resolution SEM imagines of the NFC aerogels exhibit a fibrillar structure while SP aerogels display leaf-like features (see Figure S1 of the Supporting Information). The composite aerogel systems (50:50 SP–NFC) exhibit intermediate morphological features when compared to aerogels with neat NFC or SP; fibrous as well as small leaf-like structures are observed.

The BET surface area of NFC aerogels is 1.90 ± 0.07 m^2/g noting that such values have proven to be highly dependent on the method used in aerogel synthesis; for example, there are reports of NFC aerogels with surface areas of 20 and 70 m^2/g produced by vacuum drying or fast freezing (Paakko et al. 2008) and values between 153 and 249 m^2/g when solvent exchange is followed by fast freezing (Sehaqui 2011). The comparably low surface obtained in the present study results from the rate of solvent crystallization. The slow cooling and freezing rates used in this work allowed large, defect-free materials which are characterized from the larger ice crystals formed from water leading to larger pores and lower surface areas. The surface area decreases even more when the SP loading increases (Fig. 2). This effect can be explained by (1) the lower hydrophilicity of SP compared with NFC, which leads to solute exclusion when ice crystals are formed during freezing and, by (2) the affinity between cellulose nanofibrils and the protein that produce a more dense structure and reduce the resultant material porosity. In addition, the

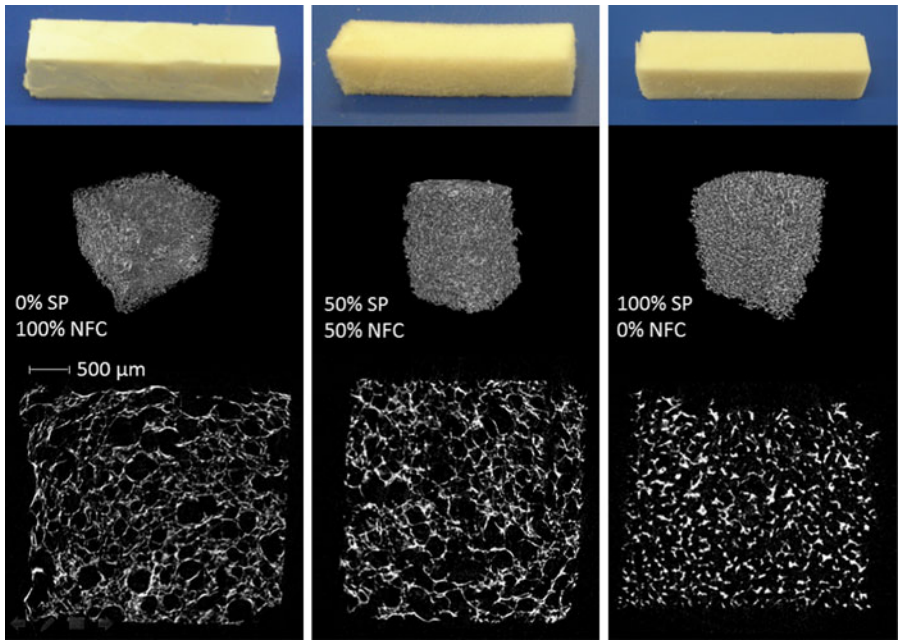

Fig. 1 *Upper section* SP–NFC composite aerogels of a few selected compositions: 100 % NFC, 50:50 SP–NFC and 100 % SP. *Lower section* tomography images (×30) of cubic sections of the respective aerogel

inherently porous nature of NFC is in contrast to that of SPs that are less amenable to the formation of higher order structures. We note that if materials with high surface areas are required for any given application, fast freezing techniques or supercritical drying may be required; a balance needs to be found since these procedures may offset the advantage of the low cost involved by the use of inexpensive SPs.

Density and porosity

The density of the SP–NFC based aerogels was in the range of 0.111–0.115 g/cm^3; these values are directly related to the solids content of the precursor aqueous gel before freezing. Because the initial solids content of the gels was 8 % in all cases, a minimum density of 0.08 g cm^{-3} was expected. Thus, the larger experimental density of the aerogels obtained can be explained by the contraction of the solid upon drying. In passing, we note that the initial solids content (8 %) was selected based upon the minimum SP concentration that generated hydrogels after acid treatment and were viscous enough to withstand the drying stresses. As a reference, it is noteworthy that the density of commercial porous materials such as Styrofoam is approximately 0.1 g cm^{-3}, similar to that of the obtained aerogels. Composite SP–NFC aerogels of lower density can be produced by employing lower initial solids contents in the precursor hydrogels. However, the present discussion is limited to systems produced from gels from a total initial solids content fixed at 8 %.

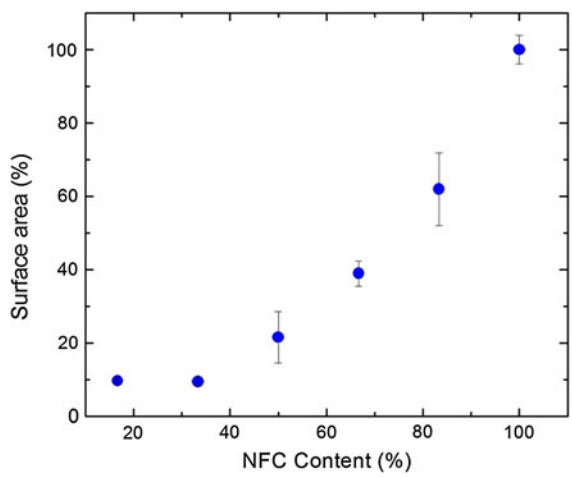

Fig. 2 BET surface area of SP–NFC aerogels relative to that for neat NFC aerogels (100 %). The sensitivity of the equipment used is compromised at low surface areas and therefore only data for up to ca. 83 % SP (17 % NFC) content is presented

The pore volume of the aerogels was calculated from the measured apparent density and that of solid NFC and SP, using theoretical values for the densities of SP isolate (1.39 g/cm^3) and NFC (1.55 g/cm^3). Porosities of 92.7 and 92.0 % were calculated for aerogels from neat NFC and neat SP, respectively. It can be expected that different pore types in the aerogels can be produced: those from dispersed air bubbles with entrained air introduced before drying and those generated after sublimation of ice crystals upon freeze drying. Blomfeldt et al. (2010) fabricated porous materials from alkaline wheat protein dough by using a chopper mixer and studied the reinforcement effect of bacterial cellulose while introducing plasticization by the use of glycerin. In contrast to the procedure used by these authors of introducing air bubbles before water removal (20–40 % in volume), the current systems involved minimal effects of dispersed air, mainly because of the very low shear used (manual mixing). This was an intended consequence because air bubble incorporation was minimized in order to account for the contribution of solvent removal. The final porosity is highly dependent on the mixing procedure and equipment used; thus, changes in density can be obtained by the judicious selection of the mixing protocol.

The use of SP implies some restrictions in the procedure used to obtain the aerogels, due the inherent rheological behavior of the precursor hydrogels: they can flow when vacuum or fast freezing is applied (fast expansion of the material generates flow while it is being frozen), which produce major defects in the structure of the aerogel. The use of vacuum drying and fast freezing refrigerants (liquid nitrogen, liquid propane, or dry ice/acetone) can be considered in the synthesis of pure NFC aerogels (Paakko et al. 2008), but adjustment of the rheology of SP gels is required if these techniques are to be used in the production of defect-free, porous materials with high mechanical integrity.

Ice crystals tend to solidify preferentially on the surface of already formed ice; consequently, when heterogeneous aqueous systems are frozen, water tends to crystalize forming channels that follow the temperature gradients inside the material (Li et al. 2012). Therefore, this mechanism can be used to obtain organized structures. With careful control of temperature gradients, the production of porous structures with superior strength can be facilitated as has been reported in the case of ceramic materials (Munch et al. 2008). However, related channel-like structures make the material weak and heterogeneous.

For the reasons discussed above, slow freezing was used whereupon temperature gradients and channel formation were minimized. Typically, the exterior walls of the molds are colder than the contained SP and/or NFC and therefore a thin ice film can be formed on the surfaces, where the initial freezing occurs. This phenomenon helps to keep the protein or NFC out of direct contact with the interior walls of the mold, facilitating aerogel extraction. However, it was noted that the final shape of the porous material may not resemble that of the mold used, especially if low solids gels are employed. In such a case it was found that this issue can be overcome by increasing the ionic strength of the system before freezing. All in all, the procedure described here for the fabrication of SP-based aerogels, especially the use of slow freezing before drying, was found to be very convenient to resolve most of the difficulties observed and to minimize defects that are otherwise encountered if alternative fabrication methods are used.

Equilibrium moisture

The aerogels absorb water from humid air, the extent of which depends on the composition, as can be observed in Fig. 3. The sorption phenomenon is somewhat similar for all aerogel compositions (around 4–5 % with respect to the dry material); however, a small but clear increase in moisture sorption capacity was observed in aerogels as the SP loading was increased. Water uptake from the air can be explained by the inherent affinity of both SP and cellulose for water. It can be argued that sorption from SP-rich aerogels could be limited due to the presence of about 18 % hydrophobic residues in the biomacromolecules (Endres 2001). However, the contribution from hydrophilic residues tends to dominate. Furthermore, the observed limited changes in moisture absorption may suggest that morphological effects may compensate for any hydrophilicity loss when SP is used, as can be derived from the change in the porous or capillary structure of the system.

Mechanical properties

The results from the mechanical tests conducted with the aerogels in compression mode are summarized in

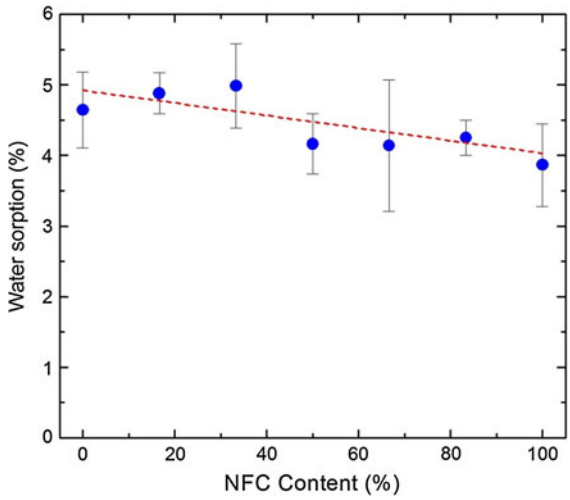

Fig. 3 Water sorption capacity from conditioned air (23 °C, 50 % relative humidity) after 48 h equilibrium

Fig. 4. Figure 4a shows the compressive stress–strain curves for aerogels ranging from 100 % SP to 100 % NFC. The aerogels consisting of 100 % SP displayed the characteristic compressive stress–strain behavior of a cellular material; an initial, small, elastic region is followed by an extensive plateau region, were the stress rises only slightly with increasing deformation, probably due to the collapse of the structure. This plateau region is followed by sudden increase in stress occurring at approximately 50 % strain indicating complete collapse of the structure and the initiation of densification. In contrast, NFC-based and composite aerogels with SP concentration up to 68 % exhibited remarkably similar mechanical properties, as judged by the compression stress–strain curves that revealed an average tensile modulus of 4.4 MPa.

The stiffness of the NFC and composite aerogels is clearly much greater than that of the 100 % SP aerogel as may be observed from the significantly larger slope of the initial portion of the stress–strain curves. This is not unexpected given the high stiffness of NFC and differences between the two microstructures. Aerogels with 83.3 % SP compared with 100 % SP content, exhibit intermediate behavior with a larger elastic region and a less distinctive plateau that accompanies the collapse of the pores followed by a final compression zone that is characteristic of a collapsed, compacted material. From these results it can be concluded that NFC works as a reinforcement agent even when applied at low concentrations (for SP contents as high as ca. 70 %).

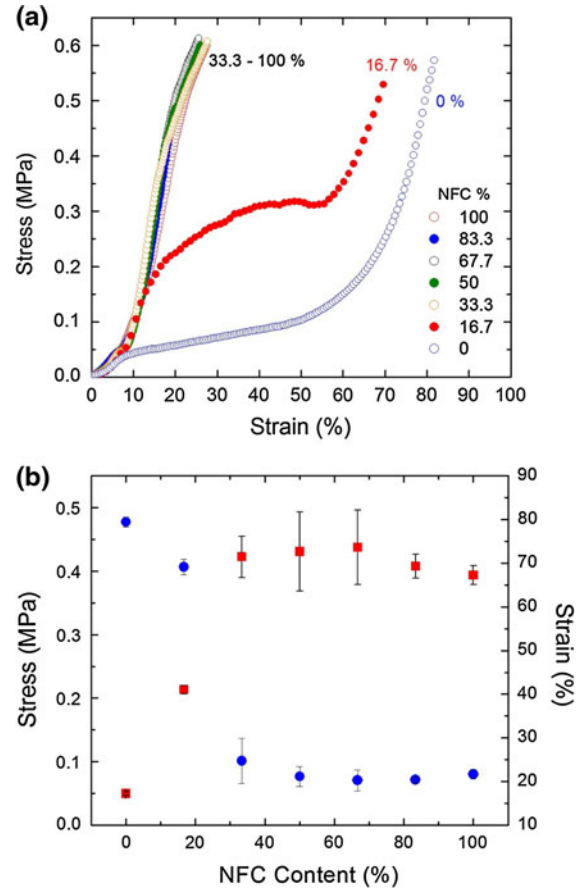

Fig. 4 Compression stress–strain curve for aerogels with different composition (**a**). Shown also is the measured stress at 18 % strain as a function of SP content (**b**, *square symbols*) and the deformation (strain) measured at 0.5 MPa compression (**b**, *circle symbols*). The standard deviations were obtained from measurements performed on at least three samples at the given condition

To put these results in a different light, it is possible to replace the more expensive fibrillar cellulose materials with SPs thus endowing the system with interesting chemical features *while maintaining a high compression modulus at approximately the same levels of the cellulose, but with high SP loading*.

Because the compression behaviors of the NFC-rich aerogels are very similar and the profiles are difficult to differentiate, Fig. 4b shows the stress required to produce 18 % compressive strain in aerogels containing various ratios of NFC to SP. Similarly, Fig. 4b shows the strain obtained at 0.5 MPa stress in aerogels containing various ratios of NFC to SP. It can be observed that aerogels with SP

concentrations up to ca. 70 % (30 % NFC) have a mechanical performance similar to that of aerogels produced from pure (100 %) NFC *which is a remarkable finding given the actual proportions of materials in the composite*. Because NFC can form very strong aerogels possessing very high inherent mechanical properties (elastic modulus around 140 GPa and tensile strength between 2 and 6 GPa) (Nakagaito et al. 2005), it can be concluded that the reduction in mechanical performance, related to SP addition can be ascribed to its distinctive effect on the morphology of the system, as illustrated in Fig. 1. From the tomographic images, it can be concluded that even though both NFC and SP tend to form open cell porous materials, the cells formed by SP tend to be more interconnected and the edges of the pores tend to be less pronounced. The lower strength of SP-based aerogels, thus, is not only explained by the lower inherent strength of SP relative to NFC, but also by the lower energy dissipation capacity of the material caused by its morphology. The morphology effect is more evident when aerogels with SP composition between 0 and 67.7 % SP (NFC content of 33.3–100 %) are compared: these materials have similar performance even though their components have different strengths, highlighting the contribution of the morphology to mechanical strength.

Liquid sorption

The aerogels adsorb water by a wicking mechanism upon contact with the fluid (Fig. 5). Aerogels of pure NFC absorbed water very rapidly. The sorption rate decreased as NFC was replaced by SP. This behavior can be explained, in part, by the differences in chemical composition: NFC contain a high density of hydroxyl groups with affinity for water, while SP is composed of approximately 18 % of hydrophobic residues (Endres 2001). BET experiments generated values of the constant "C" for the affinity (heat of adsorption) between the solid and the adsorbate (N_2 molecules); C was observed to reduce monotonically as the SP content increased, however, it is difficult to correlate such trend with the hydrophobic–hydrophilic interaction at the solid–liquid interface. Finally, we note that capillary ascension in porous solids is largely dependent on the pore's geometry and in particular on the pore diameters, which should be hence considered for a more complete understanding of the data.

Immersion experiments in water were also performed (Fig. 6); swelling and consequently higher loading capacity was observed in SP-rich aerogels. Both swelling and loading capacity were reduced with NFC content as a result of a more rigid material in the wet state as consequence of more inter-fibrillar interactions of NFC. We note that the pH of the solution after immersion in water was lowered as consequence of HCl release (future work should consider the stability of cellulose over time and may

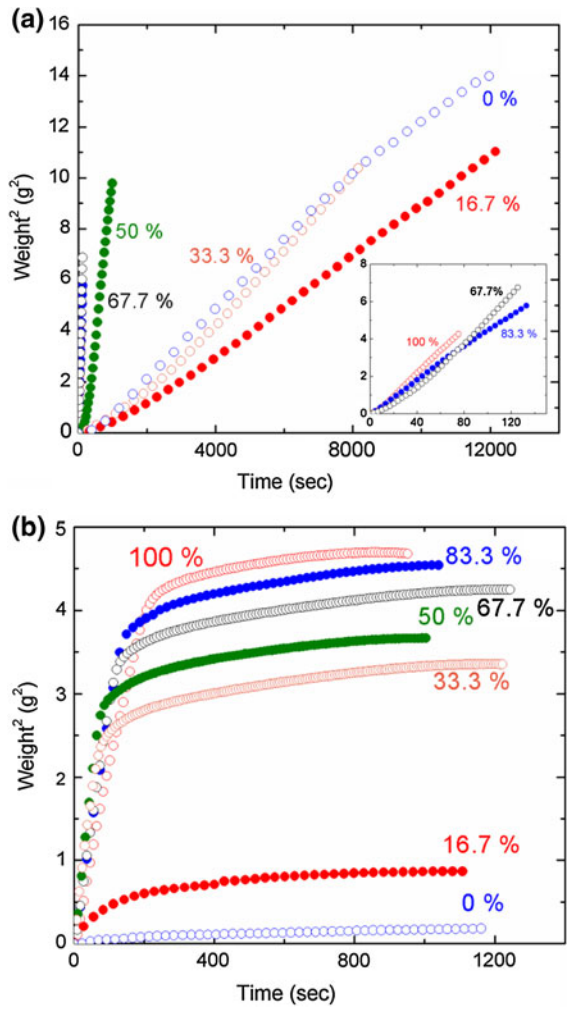

Fig. 5 Wicking of aerogels as measured by water (**a**) and hexane (**b**) uptake as a function of contact time. The amount of fluid uptake is represented as the *square* of weight gained by the aerogel according to the Lucas–Washburn equation. The *inset* in **a** correspond to short wicking times where the differences of aerogel sorption with NFC loading from 83.3 to 100 % can be better observed. The % values indicated in the figures correspond to the NFC% in the aerogel based on total dry mass

require the use of volatile acids that can be easily removed during freeze drying).

Wicking and immersion experiments were also performed with nonpolar hexane. For all aerogel compositions, fluid sorption was faster compared to that measured for water. This is in part because of the low viscosity of hexane (294 μPa s). In addition some further differences in the adsorption rate can be highlighted: fluid sorption rate increases with SP content, then decreases when SP composition reaches 67 % concentration. This behavior is explained by the increasing amount of hydrophobic residues that may interact with the nonpolar hexane; a further reduction of fluid sorption rate can be caused by morphological differences in the materials. During the wicking test (Fig. 5), the hexane advanced through the capillary structure of the aerogel until reaching a maximum height, when gravitational forces were dominant and prevented further ascension; from visual inspection it was observed that this maximum advancing height decreased with SP loading, as a consequence of the morphology induced in the sample.

The results of hexane sorption by immersion dependent on the NFC content are shown in Fig. 6. Unlike water, hexane did not cause any swelling in any of the aerogel samples, and as a consequence, negligible variations in nonpolar fluid capacity load were observed.

In closing, it is demonstrated that SP aerogels can be produced by taking advantage of the reinforcing effect of NFC and offer possibilities for deployment in given applications. Optimization of the manufacture procedures can be considered in order to obtain aerogels that tailor given applications, for example, those requiring high surface area. Their low density and good mechanical properties make them interesting candidates for potential applications which may include packaging, thermal and acoustic insulation, transport media, etc. Their stability after water and hexane sorption suggests that it is also possible to use them in different media. Finally, their overall amino acid-based composition allows chemical modification for a multiplicity of specific functions to be performed.

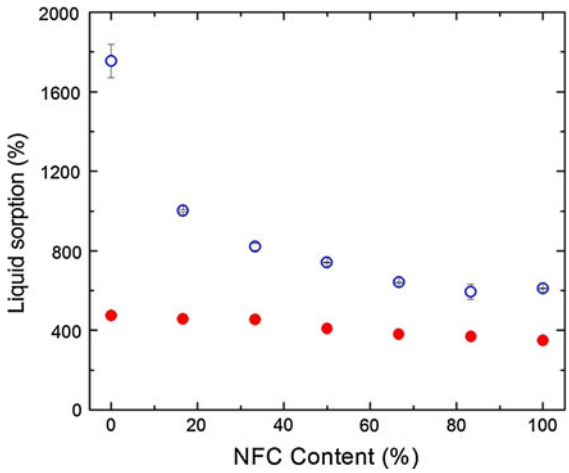

Fig. 6 Water (*blue*) and hexane (*red*) sorption by immersion. (Color figure online)

Conclusions

It has been shown that it is possible to obtain porous materials by freeze drying denatured SPs in acidic media while their mechanical properties can be improved by utilizing NFC. To avoid channel formation caused by directional freezing, the temperature gradients through the material need to be minimized. The developed aerogels can absorb water and other solvents while maintaining their integrity; their solvent loading capacity is affected by swelling, which decreases when NFC is used. High soy protein content decreases the water sorption rate but increases the maximum loading capacity. Finally, it has been shown that these materials can display mechanical properties on par with those of NFC-based gels with a relatively minor contribution of NFC to the SP matrix.

Acknowledgments LignoCell project, supported by the Finnish Funding Agency for Technology and Innovation (TEKES) and Academy of Finland is gratefully acknowledged. The authors are also thankful for funding support provided by the United Soybean Board (USB) under project numbers 2490 and 2466. We are grateful to Mika Kankkunen from Stora Enso for his help in performing tomography analyses. We appreciate very much the discussions with Prof. Olli Ikkala (Aalto University) and his group on the manufacture of cellulosic aerogels. Also, discussions with Dr. Joseph Jakes (Forest Products Lab, USDA) are gratefully acknowledged.

References

Blomfeldt TOJ, Olsson RT, Menon M, Plackett D, Johansson E, Hedenqvist MS (2010) Novel foams based on freeze-dried renewable vital wheat gluten. Macromol Mater Eng 295:796–801. doi:10.1002/mame.201000049

Endres JG (2001) Soy protein products: characteristics, nutritional aspects, and utilization. AOCS Press, Champaign, IL

Goli KK, Rojas OJ, Oezcam AE, Genzer J (2012) Generation of functional coatings on hydrophobic surfaces through deposition of denatured proteins followed by grafting from polymerization. Biomacromolecules 13:1371–1382. doi:10.1021/bm300075u

Granström M, Pääkkö MKN, Jin H, Kolehmainen E, Kilpeläinen I, Ikkala O (2011) Highly water repellent aerogels based on cellulose stearoyl esters. Polym Chem 2:1789–1796. doi:10.1039/c0py00309c,a

Gurav JL, Jung I, Park H, Kang ES, Nadargi DY (2010) Silica aerogel: synthesis and applications. J Nanomater 409310. doi:10.1155/2010/409310

Jin H, Kettunen M, Laiho A, Pynnonen H, Paltakari J, Marmur A, Ikkala O, Ras RHA (2011) Superhydrophobic and superoleophobic nanocellulose aerogel membranes as bioinspired cargo carriers on water and oil. Langmuir 27:1930–1934. doi:10.1021/la103877r

Kettunen M, Silvennoinen RJ, Houbenov N, Nykanen A, Ruokolainen J, Sainio J, Pore V, Kemell M, Ankerfors M, Lindstrom T, Ritala M, Ras RHA, Ikkala O (2011) Photoswitchable superabsorbency based on nanocellulose aerogels. Adv Funct Mater 21:510–517. doi:10.1002/adfm.201001431

Khalil HPSA, Bhat AH, Yusra AFI (2012) Green composites from sustainable cellulose nanofibrils: a review. Carbohydr Polym 87:963–979. doi:10.1016/j.carbpol.2011.08.078

Koga H, Azetsu A, Tokunaga E, Saito T, Isogai A, Kitaoka T (2012) Topological loading of Cu(I) catalysts onto crystalline cellulose nanofibrils for the Huisgen click reaction. J Mater Chem 22:5538–5542. doi:10.1039/c2jm15661j

Korhonen JT, Kettunen M, Ras RHA, Ikkala O (2011) Hydrophobic nanocellulose aerogels as floating, sustainable, reusable, and recyclable oil absorbents. ACS Appl Mater Interfaces 3:1813–1816. doi:10.1021/am200475b

Li WL, Lu K, Walz JY (2012) Freeze casting of porous materials: review of critical factors in microstructure evolution. Int Mater Rev 57:37–60. doi:10.1179/1743280411Y.0000000011

Luyten J, Mullens S, Thijs I (2010) Designing with pores—synthesis and applications. KONA Powder Part J 28:131–142

Menzel N, Ortel E, Kraehnert R, Strasser P (2012) Electrocatalysis using porous nanostructured materials. ChemPhysChem 13:1385–1394. doi:10.1002/cphc.201100984

Munch E, Launey ME, Alsem DH, Saiz E, Tomsia AP, Ritchie RO (2008) Tough, bio-inspired hybrid materials. Science 322:1516–1520. doi:10.1126/science.1164865

Nakagaito A, Iwamoto S, Yano H (2005) Bacterial cellulose: the ultimate nano-scalar cellulose morphology for the production of high-strength composites. Appl Phys A Mater Sci Process 80:93–97. doi:10.1007/s00339-004-2932-3

Olsson RT, Samir MASA, Salazar-Alvarez G, Belova L, Strom V, Berglund LA, Ikkala O, Nogues J, Gedde UW (2010) Making flexible magnetic aerogels and stiff magnetic nanopaper using cellulose nanofibrils as templates. Nat Nanotechnol 5:584–588. doi:10.1038/NNANO.2010.155

Paakko M, Vapaavuori J, Silvennoinen R, Kosonen H, Ankerfors M, Lindstrom T, Berglund LA, Ikkala O (2008) Long and entangled native cellulose I nanofibers allow flexible aerogels and hierarchically porous templates for functionalities. Soft Matter 4:2492–2499. doi:10.1039/b810371b

Reddy N, Yang Y (2011) Potential of plant proteins for medical applications. Trends Biotechnol 29:490–498. doi:10.1016/j.tibtech.2011.05.003

Renkema J, Lakemond C, de Jongh H, Gruppen H, van Vliet T (2000) The effect of pH on heat denaturation and gel forming properties of soy proteins. J Biotechnol 79:223–230. doi:10.1016/S0168-1656(00)00239-X

Salas C, Rojas OJ, Lucia LA, Hubbe MA, Genzer J (2012) Adsorption of glycinin and beta-conglycinin on silica and cellulose: surface interactions as a function of denaturation, pH, and electrolytes. Biomacromolecules 13:387–396. doi:10.1021/bm2014153

Sarmadi BH, Ismail A (2010) Antioxidative peptides from food proteins: a review. Peptides 31:1949–1956. doi:10.1016/j.peptides.2010.06.020

Sehaqui H, Zhou Q, Berglund LA (2011) High-porosity aerogels of high specific surface area prepared from nanofibrillated cellulose (NFC). Compos Sci Technol 71:1593–1599. doi:10.1016/j.compscitech.2011.07.003

Song F, Tang D, Wang X, Wang Y (2011) Biodegradable soy protein isolate-based materials: a review. Biomacromolecules 12:3369–3380. doi:10.1021/bm200904x

Wagner J, Gueguen J (1999) Surface functional properties of native, acid-treated, and reduced soy glycinin. 2. Emulsifying properties. J Agric Food Chem 47:2181–2187. doi:10.1021/jf9809784

Washburn E (1921) The dynamics of capillary flow. Phys Rev 17:273–283. doi:10.1103/PhysRev.17.273

Zhang Y, Riduan SN (2012) Functional porous organic polymers for heterogeneous catalysis. Chem Soc Rev 41:2083–2094. doi:10.1039/c1cs15227k

Zhong Z, Sun XS, Wang D (2007) Isoelectric pH of polyamide–epichlorohydrin modified soy protein improved water resistance and adhesion properties. J Appl Polym Sci 103:2261–2270. doi:10.1002/app.25388